

Identification of Magnetic Nanoparticles for Combined Positioning and Lentiviral Transduction of Endothelial Cells

Daniela Wenzel · Sarah Rieck · Sarah Vosen · Olga Mykhaylyk · Christina Trueck · Dietmar Eberbeck · Lutz Trahms · Katrin Zimmermann · Alexander Pfeifer · Bernd K. Fleischmann

Received: 3 August 2011 / Accepted: 13 December 2011 / Published online: 10 January 2012
© Springer Science+Business Media, LLC 2012

ABSTRACT

Purpose The combination of magnetic nanoparticles (MNPs) with a magnetic field is a powerful approach to enable cell positioning and/or local gene therapy. Because physical requirements for MNPs differ between these two applications we have explored whether the use of different MNPs can provide site-specific positioning combined with efficient viral transduction of endothelial cells (ECs).

Methods A variety of MNPs was screened for magnetic cell labeling and lentivirus binding. Then two different MNPs were chosen and their combined application was evaluated regarding EC magnetization and transduction efficiency.

Results The combined use of PEI-Mag2 and NDT-Mag1 particles provided both efficient lentiviral transduction and high magnetic responsiveness of ECs that could be even retained within the vascular wall under flow conditions. The use of these MNPs did not affect biological characteristics of ECs like surface marker expression and vascular network formation. Importantly, with this method we could achieve an efficient functional overexpression of endothelial nitric oxide synthase in ECs.

Conclusions The application of two different MNPs provides optimal results for magnetic labeling of ECs in combination with viral transduction. This novel approach could be very useful for targeted gene therapy *ex vivo* and site-specific cell replacement in the vascular system.

KEY WORDS endothelial cell replacement · gene transfer · lentiviral transduction · magnetic cell labeling · magnetic nanoparticles

ABBREVIATIONS

bPAECs	bovine pulmonary endothelial cells
CMV	cytomegalovirus
ECs	endothelial cells
eGFP	enhanced green fluorescent protein
eNOS	endothelial nitric oxide synthase
Fe	iron
LV	lentivirus
MNPs	magnetic nanoparticles
MOI	multiplicity of infection
MPS	magnetic particle spectroscopy
NDT/PEI (0.04)	NDT-Mag1/PEI-Mag2 at a ratio of 0.04 pg Fe/VP
NDT/PEI (25)	NDT-Mag1/PEI-Mag2 at a ratio of 25 pg Fe/cell
PECAM	platelet endothelial cell adhesion molecule
VP	virus particle

INTRODUCTION

Magnetic nanoparticles (MNPs) are currently utilized for a variety of applications in biomedicine. They are used as contrast agents to obtain a high spatial resolution in mag-

Electronic supplementary material The online version of this article (doi:10.1007/s11095-011-0657-5) contains supplementary material, which is available to authorized users.

D. Wenzel (✉) · S. Rieck · S. Vosen · B. K. Fleischmann
Institute of Physiology I, University of Bonn
Sigmund-Freud-Str.25
53127 Bonn, Germany
e-mail: dwenzel@uni-bonn.de

O. Mykhaylyk
Institute of Experimental Oncology, TU München
Munich, Germany

C. Trueck · K. Zimmermann · A. Pfeifer
Institute of Pharmacology and Toxicology, University of Bonn
Bonn, Germany

D. Eberbeck · L. Trahms
Physikalisch-Technische Bundesanstalt
Berlin, Germany

netic resonance imaging (MRI) and can accumulate in tumors or atherosclerotic plaques enabling site-specific disease detection (1,2). Besides diagnostic applications, MNPs can be also employed for therapeutic purposes. For example, tumor tissue has been loaded with MNPs and thereafter been exposed to high frequency magnetic fields resulting in local hyperthermia and tumor regression (3). Moreover, also site-specific drug delivery can be accomplished with MNPs by applying external magnetic field gradients to enrich drug/MNP complexes at the target site (4). In addition, MNPs are efficiently used for DNA, protein or cell labeling and their subsequent purification in a magnetic field (5–8). Cell labeling with MNPs has also been exploited for *ex vivo* tissue engineering strategies: MNPs have been shown to support the construction of keratinocyte sheets (9) and the coating of synthetic vascular grafts with endothelial cells (ECs) (10,11). Moreover, gene delivery in cells and tissues could be improved by non-viral or viral vectors associated with MNPs, so-called magnetofection (12–14).

We have shown in an earlier study that ECs could be efficiently transduced with lentivirus (LV)/MNP complexes even at low temperature *in vitro* as well as under flow conditions *ex vivo* (15). In addition, LV and MNPs can be also utilized to combine gene therapy with cell replacement. However, a major limitation of combining lentiviral transduction with cell positioning is that no single type of MNPs has the physico-chemical characteristics required to provide optimal results for both these applications. In fact, MNPs with a high magnetic moment are best suited for cell positioning, whereas these often do not allow for optimal virus binding and *vice versa*. We therefore sought to combine different types of MNPs to provide efficient viral transduction of ECs and retention at the vascular wall under flow conditions.

MATERIALS AND METHODS

Cell Culture

Bovine pulmonary arterial endothelial cells (bPAECs) were obtained from Provitro (Berlin, Germany). They were cultivated in endothelial cell growth medium (ECGM) as recommended by the manufacturer and used until passage 8.

Magnetic Labeling of bPAECs and Magnetic Rack Experiments

The generation of PEI-Mag2 and NDT-Mag1 particles containing magnetite cores has been previously described (16); the characteristics of magnetic nanoparticles (MNPs) used for screening are shown in Supp. Table I. For magnetic labeling experiments 150,000 cells/well were seeded in a 6-

well plate. The required amount of MNPs was suspended in 1 ml of Hank's Balanced Salt Solution with calcium and magnesium (HBSS⁺⁺, Invitrogen, Darmstadt, Germany). Cells were washed once with HBSS⁺⁺ and then incubated with MNP suspension for 30 min on a magnetic plate (Chemicell, Berlin, Germany) at 37°C. Afterwards MNP suspension was replaced with ECGM.

Twenty four hours after labeling cells were detached using Accutase (Provitro, Berlin, Germany) and passed through a magnetic rack. The rack consists of a custom-built acrylic glass block with slots for 1.5 ml reaction tubes. The slots contain two cuboid-formed permanent magnets (N44, N50, www.magnet-shop.net, Cat. No.: QM-20x05x02-N, QM-10x04x02-G) closely attached to the tube wall ranging from top to bottom. When a suspension of cells is transferred to the wall of a reaction tube near the magnet labeled cells are retained at the wall, non-labeled cells are collected at the bottom of the tube. The amount of retained magnetic cells and non-magnetic cells in the effluent was determined by cell counting.

Lactate Dehydrogenase (LDH) Assay

The LDH assay was applied to exclude a toxic effect of cell loading with MNPs. Therefore 20,000 cells were plated in a 24-well plate and magnetically labeled with MNPs as described above. After approximately 18 h the cell culture supernatant was centrifuged to pellet cell debris and the supernatant was analyzed using the LDH assay according to the manufacturer's instruction (Cytotoxicity Detection kit plus, Roche Diagnostics, Indianapolis, IN, USA).

Virus Binding Curves

Complexes of MNPs and lentiviruses (LVs) were generated in HBSS⁺⁺, then the suspension was transferred to a 24-well plate. During the incubation time of 30 min at 4°C on a magnetic plate, MNP-bound LVs sedimented within the wells. After that, the uncomplexed LVs in the supernatant were quantified by ELISA detecting the lentiviral capsid protein p24 (RETRO-TEK HIV-1 p24 Antigen ELISA, Zeptrometrix Corporation Buffalo, NY, USA). As control, suspensions with LVs but without MNPs were used. To calculate the MNP-bound LVs, LVs contained in the supernatant after complexation were subtracted from the LVs in the supernatant of controls and expressed relative to controls.

Magnetic Responsiveness Measurements

Magnetic responsiveness measurements were performed according to the published protocol by Mykhaylyk *et al.* (17). Briefly, suspensions of magnetically labeled cells were

transferred into a well-defined inhomogeneous magnetic gradient field. This field was generated by two mutually attracting packs of four quadrangular NdFeB magnets symmetrically positioned on each side of a cuvette holder. Then the time course of the optical density or turbidity of the suspensions was measured in a spectrophotometer. From the clearance velocity of the suspension the magnetic moment and iron content of the cells were calculated as described by Wilhelm *et al.* (18).

Magnetic Particle Spectroscopy (MPS)

Magnetic Particle Spectroscopy (MPS) measures the spectral density of the higher harmonics of the dynamic magnetization behavior of MNPs on the basis of the newly developed Magnetic Particle Imaging (MPI) (19). The samples were exposed to a strong alternating field with a strength of $\mu_0 H = 10$ mT with a frequency of $f_0 = 25$ kHz. Then the nonlinear part of magnetization of MNPs produces amplitudes of higher harmonics with frequencies $f_k = (2k + 1)f_0$, $k = 1, 2, 3, \dots$ in the Fourier transform of the sample's response which can be separated from the signal contribution of the base frequency f_0 by high pass filtering. Thus, the signal is very specific for MNPs as components of diamagnetic and paramagnetic parts of the samples (e.g. tissue, cell medium, blood) do not contribute to the uneven higher harmonics because they have a linear magnetization behavior in the present field range.

The sensitivity of the measurement strongly depends on the kind of the MNPs, where MNPs with a high magnetic moment produce high amplitudes due to their non-linear magnetization behavior. For NDT-Mag1 and PEI-Mag2 the detection limit amounts to 0.01 μg and 0.1 μg for A_3 and A_5 , respectively.

In order to quantify the MNPs within the cell suspensions, 150 μl of the cell suspensions as well as a reference sample containing a known amount of the MNPs from the same flask used for the transduction are measured by the MP-spectrometer. For the quantification we used the two strongest amplitudes A_3 and A_5 . Then we calculated the amount of iron within the sample according to $m(\text{Fe}) = m_{\text{Ref}}(\text{Fe}) \cdot (A_3/A_{3,\text{Ref}} + A_5/A_{5,\text{Ref}})/2$. The measurement uncertainty of the individual samples was estimated by the difference according to $u(m(\text{Fe})) = m_{\text{Ref}}(\text{Fe}) |A_3/A_{3,\text{Ref}} - A_5/A_{5,\text{Ref}}|/2$.

Transduction of bPAECs

Self-inactivating LVs containing a CMV-driven eGFP or eNOS-IRES-eGFP expression cassette were produced and biological virus titers determined as previously described (20). The physical titers were calculated from concentrations of reverse transcriptase according to Trueck *et al.* (Trueck,

Zimmermann *et al.*, this issue). Biological and physical CMV-eGFP titer was 7.48×10^9 infectious particles (IP)/ml and 3.25×10^{10} viral particles (VP)/ml, respectively. Biological and physical CMV-eNOS-IRES-eGFP titer was 6.98×10^9 IP/ml and 1.99×10^{11} VP/ml, respectively. Lentiviral transduction was exerted at a multiplicity of infection (MOI 20).

For lentiviral transduction of bPAECs cells were either plated at a density of 150,000/well in a 6-well plate (magnetic rack, Western Blot experiments) or plated at a density of 30,000/well in a 24-well plate (qRT-PCR, immunostaining experiments). Transduction was performed in 1 ml (6-well) or 0.5 ml (24-well) of HBSS⁺⁺. LV was either diluted in HBSS⁺⁺ or incubated for 20 min at room temperature with PEI-Mag2 or NDT-Mag1 in HBSS⁺⁺ resulting in 0.04 pg Fe/VP or 25 pg Fe/cell. Transduction was performed in HBSS⁺⁺ for 30 min at 37°C in an incubator using a magnetic plate (Chemically, Berlin, Germany). Lentiviral transduction over night was performed with LV in ECGM for at least 12 h at 37°C. For combined magnetic cell labeling and lentiviral transduction bPAECs were magnetically labeled with a suspension of 25 pg Fe/cell NDT-Mag1 in HBSS⁺⁺ on a magnetic plate for 30 min at 37°C followed by transduction with complexes of LV and 0.04 pg Fe/VP PEI-Mag2 12 h later.

Analysis of Transduction Efficiency

For analysis of transduction efficiency fluorescence pictures of transduced and fixated bPAECs were obtained by the Axio Observer Z1 equipped with a MosaiX module (Zeiss, Jena, Germany). Nuclei and eGFP positive cells were counted using the cell counter plug-in from WCIF Image J.

QRT-PCR

Total RNA from bPAECs was extracted with the RNeasy Micro Kit (Qiagen, Hilden, Germany). CDNA was generated using SuperScript VILO cDNA synthesis kit (Invitrogen, Darmstadt, Germany). Expression of endothelial nitric oxide synthase (eNOS), eGFP and 18S rRNA was assessed by SYBR-Green quantitative real time PCR (qRT-PCR). MasterMix and pre-designed primers were obtained from QIAGEN (eNOS: QT00089033, GFP: QT01171611, 18S rRNA: QT01036875). QRT-PCR was performed using Rotor-Gene SYBR Green PCR Kit (QIAGEN, Hilden, Germany) in a Rotor Gene Q real time PCR cycler (QIAGEN, Hilden, Germany). Relative expression levels were determined with the $2^{-\Delta\Delta C_t}$ method (21).

Western Blot Experiments

For protein extraction cells were washed once with ice-cold PBS. Cell lysis was achieved by addition of cold RIPA buffer containing protease inhibitors (Roche Applied Science,

Mannheim, Germany). Lysate was frozen at -80°C , then thawed on ice and centrifuged for 10 min with 13,000 rpm at 4°C . Supernatant was transferred to a new reaction tube and protein concentration was determined using BCA Protein Assay Kit (Thermo Scientific, Rockford, USA).

SDS-PAGE was performed in a 10% polyacrylamide gel. Electrophoresis and blotting were performed as previously described (22). Antibody dilutions were applied as follows: eNOS (Santa Cruz Biotechnology, Heidelberg, Germany): 1:1000; GFP (Clontech, Saint-Germain-en-Laye, France): 1:1000; β -actin (Sigma-Aldrich, Taufkirchen, Germany): 1:20,000.

Ex Vivo Perfusion of Mouse Aortas

Studies were conducted using female CD1 wildtype mice (Charles River, Sulzfeld, Germany) and experiments were in accordance with “Principles of Laboratory Animal Care”. The animals were sacrificed at 10 weeks of age. The thoracic aortas were dissected free of fatty and connective tissue. Then arteries were cannulated on both sides and placed in an organ bath filled with Dulbecco’s Modified Eagle Medium (DMEM, GIBCO Invitrogen, Karlsruhe, Germany). The intercostal arteries were cauterized with a soldering gun. Cannulated vessels were connected to our *ex vivo* flow-loop system (15). Recirculating perfusion was performed with approximately 10 ml of DMEM and a perfusion rate of about 4.5 ml/min for a total perfusion time of 30 min. After magnetic labeling and lentiviral transduction 400,000 bPAECs were injected into the flow-loop system as a bolus. Cells were retained by two small permanent magnets (length 14 mm, diameter 4 mm) with a magnetic flux density of about 0.6 T at the surface of the magnets (15). Pictures of the whole aorta were taken directly after perfusion using a Leica MZ 16 F stereomicroscope (Microsystems GmbH, Wetzlar, Germany).

For histological sections the arteries were incubated in 4% PFA for 30 min at room temperature and then frozen at -80°C in Tissue-Tek® O.C.T. compound medium (Sakura, Zoeterwoude, Netherlands). Frozen tissue samples were sectioned into 10 μm slices using a Leica cryotome (Leica, Wetzlar, Germany).

The immunofluorescence stainings were performed using primary antibodies directed against platelet endothelial cell adhesion molecule (PECAM, 1:800, kindly provided by Dr. Newman, University of Wisconsin) and murine α -smooth-muscle-actin (1:800, Sigma Aldrich, Munich, Germany). As secondary antibodies Cy3 anti-rabbit (1:400, Dianova, Hamburg, Germany) and Alexa 647 anti-mouse (1:400, Molecular Probes, Invitrogen, Darmstadt, Germany) were used. The prussian blue staining was performed as described below.

Pictures of the labeled sections were obtained using an Axio Observer Z1 microscope (Carl Zeiss MicroImaging GmbH, Göttingen, Germany) and pictures of the prussian blue staining were taken using an Axiovert 200 microscope (Carl Zeiss MicroImaging GmbH, Göttingen, Germany).

Prussian Blue Staining

Iron staining of magnetically labeled cells was performed according to the prussian blue method. Therefore, bPAECs were fixated by 4% PFA and incubated with staining solution (5% potassium ferricyanide II solution mixed with 5% hydrochloric acid (1:1)) for 20 min. Afterwards, cells were counterstained with 0.5% eosin G solution (Carl Roth, Karlsruhe, Germany) for 5 min and mounted with entellan (Merck, Darmstadt).

Immunocytochemistry of bPAECs

To investigate the cellular expression of eNOS and PECAM in bPAECs, cells were cultivated on coverslips coated with 0.1% gelatine. After PFA fixation, cells were permeabilized with 0.2% Triton X-100 (Roth, Karlsruhe, Germany) and blocked with 5% donkey serum (Vector laboratories, Eching, Germany). Then cells were incubated for 1 h with primary antibodies anti-eNOS (1:50, BD Biosciences, Heidelberg, Germany) and anti-PECAM (1:500). As secondary antibodies Cy3 anti-mouse and Cy5 anti-rabbit (1:400, Dianova) were used. Nuclei were stained with Hoechst 3342 (1:1000, Sigma-Aldrich, Taufkirchen, Germany).

Angiogenesis Assay

To prove the angiogenic capacity of bPAECs, cells were transduced in 6-well plates (100,000 cells/well). Two days after transduction they were transferred to Matrigel-coated 24-well plates (200 μl Matrigel/well, 50,000 cells/well, BD Biosciences, Heidelberg, Germany). Pictures were taken 24 h after transfer to Matrigel.

Analysis of Nitric Oxide Synthesis

Nitric oxide synthesis of bPAECs was analyzed using a diaminofluorescein assay (DAF assay). BPAECs at passage 5 were cultivated and transduced in 6-well plates (200,000 cells/well). For DAF measurements a CMV-eNOS virus was used to prevent false positive fluorescence signals by eGFP leaking into the supernatant. The physical titer of the CMV-eNOS virus was 1.66×10^{11} VP/ml. Two days after transduction bPAECs were transferred to 24-well plates (100,000 cells/well). Three days after transduction cells were incubated with 1 μM DAF in 3 mM L-arginine in HBSS⁺⁺ for 1 h at 37°C in an incubator. As positive control

bPAECs were incubated with 100 μ M sodium nitroprusside (SNP). Supernatant was transferred to a 96-well plate and fluorescence intensity was determined using a microplate reader (excitation: 485 nm, emission: 535 nm, TECAN, Männedorf, Switzerland).

Statistical Analysis

Data are expressed as mean \pm SEM. Statistical significance was determined by one-way analysis of variance (ANOVA) and Dunnett's, Bonferroni or Tukey's post-hoc test. $P < 0.05$ was considered statistically significant.

RESULTS

In this study bovine pulmonary arterial endothelial cells (bPAECs) were used because these primary cells have certain advantages as compared to other endothelial cells (ECs): they have a high proliferation rate and therefore appear to be a sensitive cell type for potential adverse side effects of magnetic nanoparticles (MNPs).

In order to identify optimal MNPs for magnetic cell labeling and lentiviral transduction, a variety of different MNPs was screened; all MNPs tested contained a magnetite core of 9–12 nm and were coated with different surfactants and/or polymers (Suppl. Table I).

To test the capacity of MNPs to retain labeled cells in a magnetic field, suspensions of cells loaded with 10 different types of MNPs were transferred to a so-called magnetic rack (Fig. 1a); the cell suspensions were pipetted onto the edge of a small tube with an adjacent magnet and only cells with a high magnetic moment were retained whereas cells with a low magnetic moment sedimented within the tube. We found that ECs loaded with NDT-Mag1 were most efficiently retained (86%) whereas the retention rate was clearly lower for the other MNPs ranging from 30 to 70% (Fig. 1b). To test for potential cell toxicity of NDT-Mag1 a lactate dehydrogenase (LDH) assay was performed. This experiment revealed that NDT-Mag1 at a concentration of 25 pg Fe/cell was without effect in bPAECs while 100 pg Fe/cell NDT-Mag1 enhanced LDH release which is a marker for cell damage. The iron concentration causing cellular toxicity is dependent on the MNP type, because PEI-Mag2 was unlike NDT-Mag1 non-toxic at that concentration (Fig. 1c). Thus, for further experiments we have chosen 25 pg Fe/cell NDT-Mag1 for strong magnetic cell labeling of bPAECs.

Next, the MNP type with optimal lentivirus (LV) binding was determined. Therefore, NDT-Mag1 binding was directly compared to the PEI-Mag2 that showed highest LV binding capacity at low toxicity (Trueck, Zimmermann *et al.*, this issue). PEI-Mag2 was highly superior compared to NDT-Mag1 in

virus binding because PEI-Mag2 almost bound 100% of LV at a low iron to virus ratio of app. 0.04 pg Fe/virus particle (VP). In contrast, NDT-Mag1 could maximally bind about 40% of LV at a high iron to virus ratio of app. 1 pg Fe/VP. Thus, in further experiments we have performed lentiviral transduction with 0.04 pg Fe/virus particle PEI-Mag2, which enables efficient virus binding (Fig. 1d arrow).

Analysis of Magnetic Cell Labeling After Pre-loading and Lentiviral Transduction

In order to analyze the efficiency of magnetic cell labeling with NDT-Mag1, PEI-Mag2 or the combination of both particles in detail, bPAECs were loaded with MNPs or LV/MNP complexes alone for 30 min on a magnetic plate. Alternatively, loading with MNPs was followed by transduction with LV/MNP complexes. For transduction a viral vector containing a CMV promoter-driven eGFP expression cassette was applied. Prussian blue and eosin stainings were used to estimate the cellular uptake of MNPs and to label the cytoplasm in bPAECs, respectively (Fig. 2a–f). Next, the retention of the cells on the magnetic rack was tested 72 h after labeling. These experiments revealed that the MNP concentration that resulted in maximum binding of LVs to PEI-Mag2 (0.04 pg Fe/VP, i.e. 3.5 pg Fe/cell) provided only a low percentage of magnetic cells for PEI-Mag2 as well as NDT-Mag1. As expected application of 25 pg Fe/cell NDT-Mag1 produced a high amount of magnetic cells ($73.0 \pm 4.5\%$), whereas treatment of bPAECs with 25 pg Fe/cell PEI-Mag2 resulted in lower numbers of labeled cells ($46.0 \pm 3.5\%$). Interestingly, pre-loading of bPAECs with 25 pg Fe/cell NDT-Mag1 followed by application of 0.04 pg Fe/VP PEI-Mag2 for 30 min 12 h later yielded similar values as the application of 25 pg Fe/cell NDT-Mag1 alone ($64.3 \pm 2.8\%$, $p > 0.05$ vs 25 pg Fe/cell NDT-Mag1) (Fig. 2g). The high efficiency of magnetic cell labeling by NDT-Mag1 alone or NDT-Mag1 followed by lentiviral transduction with PEI-Mag2 was confirmed by magnetic responsiveness measurements (16). The average velocity of cells under the influence of a magnetic field gradient can be determined with this technique and visualized in form of a magnetic responsiveness curve (Fig. 2h); from average velocities the magnetic moments of cells can be calculated. We found that bPAECs loaded with 25 pg Fe/cell NDT-Mag1 alone or 25 pg Fe/cell NDT-Mag1 followed by 0.04 pg Fe/VP PEI-Mag2 (i.e. 3.5 pg Fe/cell) yielded a magnetic moment of $5.6 \pm 0.8 \cdot 10^{-13}$ Am² and $5.8 \pm 0.4 \cdot 10^{-13}$ Am², respectively. In contrast, cells loaded with 25 pg Fe/cell PEI-Mag2 alone only reached $2.2 \pm 0.1 \cdot 10^{-13}$ Am² (at 213 mT, $n=3$, $p < 0.05$ vs 25 pg Fe/cell NDT-Mag1 and 25 pg Fe/cell NDT-Mag1 + 0.04 pg Fe/VP PEI-Mag2). These values correspond to an iron content of about 8 pg Fe/cell ($\sim 30\%$) for 25 pg Fe/cell NDT-Mag1 or

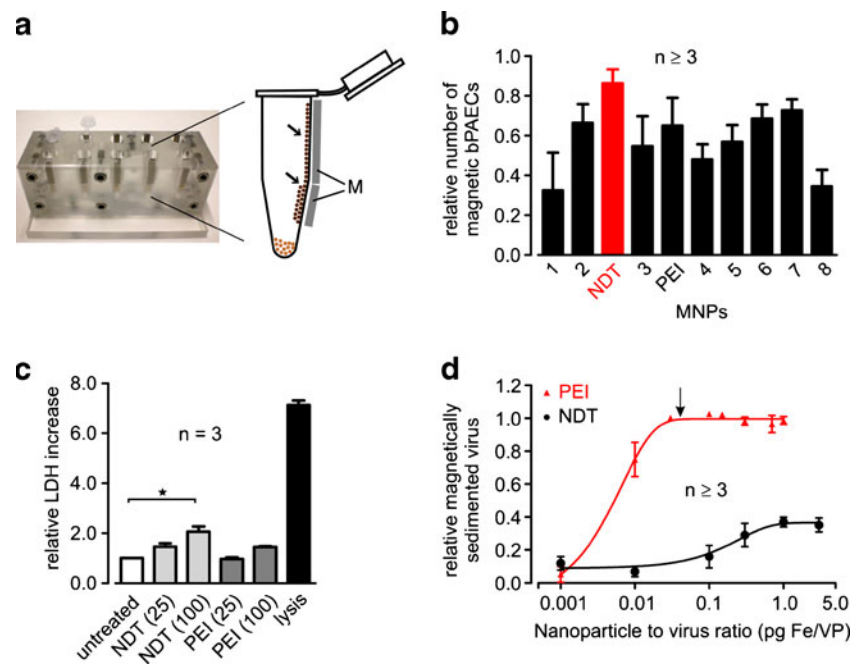


Fig. 1 Identification of suitable magnetic nanoparticles (MNPs) for magnetic cell labeling and lentiviral transduction **(a)** Picture of magnetic rack with 10 slots for small tubes (left), schematic view of tube adjacent to small magnets (M) with retained magnetic cells (arrows, right). **(b)** Cell labeling efficiency of 10 different MNPs (1–8, NDT-Mag1 (NDT) and PEI-Mag2 (PEI)) was quantified with the magnetic rack 24 h after labeling of bovine pulmonary arterial endothelial cells (bPAECs). **(c)** Lactate dehydrogenase (LDH) assay of bPAECs loaded with 25 pg Fe/cell NDT-Mag1 (NDT 25), 100 pg Fe/cell NDT-Mag1 (NDT 100), 25 pg Fe/cell PEI-Mag2 (PEI 25) and 100 pg Fe/cell PEI-Mag2 (PEI 100), cell lysis served as positive control. **(d)** Virus binding curves of NDT and PEI at different nanoparticle to virus ratios, note ratio of 0.04 pg Fe/virus particle (VP) indicated by arrow.

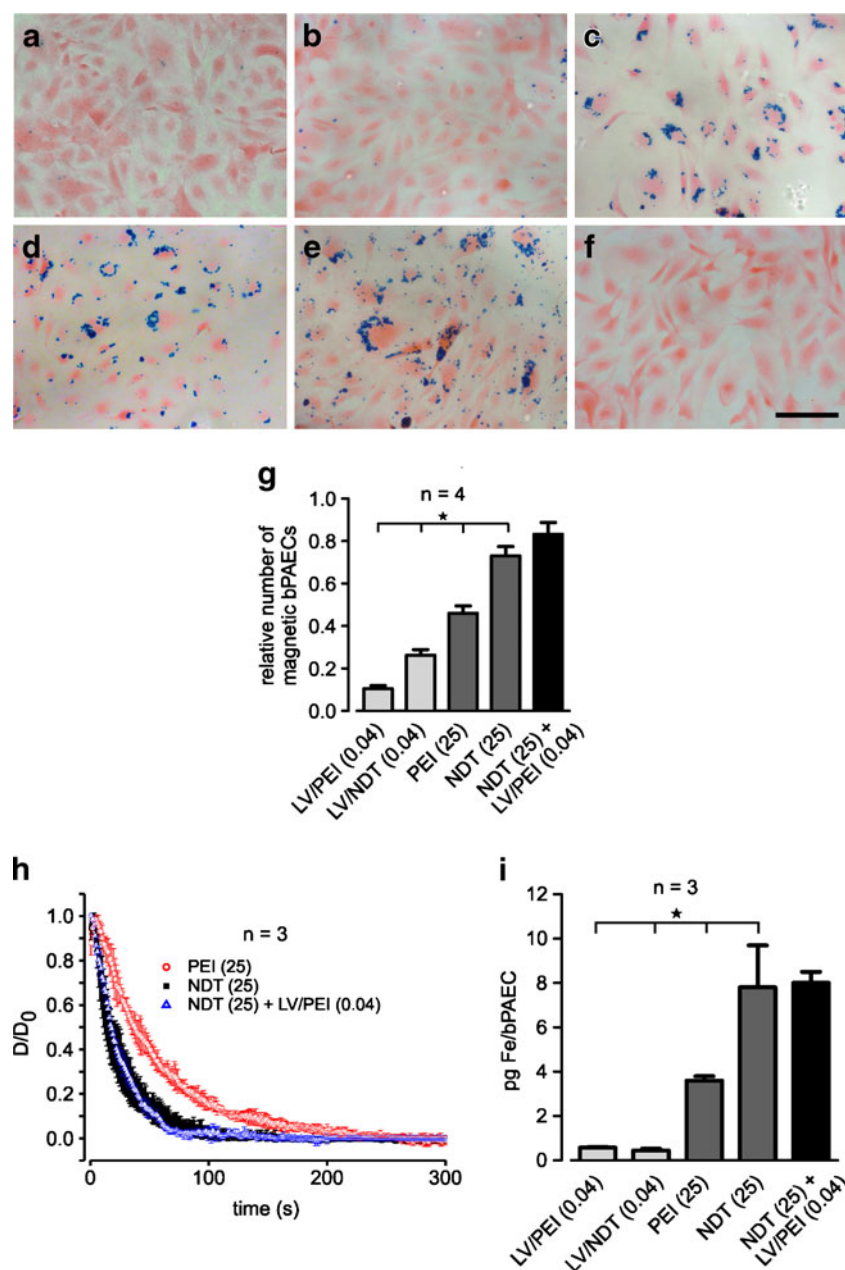
25 pg Fe/cell NDT-Mag1 + 0.04 pg Fe/VP PEI-Mag2 and only 3.5 pg Fe/cell (~15%) for 25 pg Fe/cell PEI-Mag2, (Fig. 2i). Quantitation of iron uptake in bPAECs after transduction with 0.04 pg Fe/VP NDT-Mag1 or 0.04 pg Fe/VP PEI-Mag2 by magnetic responsiveness measurements did not provide reliable results due to the limited sensitivity of this method. We therefore used magnetic particle spectroscopy (MPS), which is known to be more sensitive. The measurements revealed a 10-fold lower iron uptake after lentiviral transduction with only 0.04 pg Fe/VP (i.e. 3.5 pg Fe/cell), (Fig. 2i). More in detail, transduction with 0.04 pg Fe/VP PEI-Mag2 resulted in an uptake of 0.6 ± 0.02 pg Fe/cell (~17%) while transduction with 0.04 pg Fe/VP NDT-Mag1 ended up in 0.5 ± 0.05 pg Fe/cell (~20%). Thus, NDT-Mag1 has a higher loading capacity than PEI-Mag2 which could also explain the toxicity at 100 pg Fe/cell that was not found for PEI-Mag2 (see Fig. 1c). These data demonstrate that NDT-Mag1 particles at the high concentrations needed for magnetic labeling are superior to PEI-Mag2 due to enhanced MNP uptake and the higher magnetic moments of the cores.

Analysis of Gene and Protein Expression After Pre-loading and Lentiviral Transduction

Next we determined the efficiency of lentiviral transduction by LV/NDT-Mag1 and LV/PEI-Mag2 complexes with or without pre-loading. BPAECs were transduced applying the

eGFP virus on a magnetic plate for 30 min at room temperature; eGFP expression was analyzed 72 h later. Expression analysis with qRT-PCR indicated that 0.04 pg Fe/VP PEI-Mag2 strongly elevated eGFP mRNA expression levels 94-fold ($p < 0.05$ vs controls); this increase could not even be obtained by standard over night transduction without MNPs. Transduction with NDT-Mag1 was much less efficient than with PEI-Mag2. Importantly, pre-loading with 25 pg Fe/cell NDT-Mag1 and subsequent transduction with 0.04 pg Fe/VP PEI-Mag2 yielded similar results as transduction with 0.04 pg Fe/VP PEI-Mag2 alone suggesting that these two nanoparticles were not competing (Fig. 3a). The results were confirmed by semi-quantitative Western Blot analysis and revealed that PEI-Mag2 also strongly enhanced protein expression after lentiviral transduction independent from pre-loading with NDT-Mag1 (Fig. 3b). Finally, counting of eGFP positive cells under the microscope enabled us to quantify precisely transduction efficiencies (Fig. 3c–i). 0.04 pg Fe/VP PEI-Mag2 strongly increased the number of eGFP expressing bPAECs ($45.8 \pm 2.5\%$, $p < 0.05$ vs controls). In contrast, LV/NDT-Mag1 complexes caused only a negligible increase of eGFP positive bPAECs. Pre-loading with 25 pg Fe/cell NDT-Mag1 for magnetic cell labeling and lentiviral transduction with 0.04 pg Fe/VP PEI-Mag2 on the next day did not impair eGFP expression compared to transduction with 0.04 pg Fe/VP PEI-Mag2 complexes alone (25 pg Fe/cell NDT-

Fig. 2 Assessment of magnetic labeling of bPAECs after pre-loading and lentiviral transduction with LV/MNP complexes (**a–f**) Prussian blue (blue) and eosin (red) staining of magnetically labeled bPAECs with or without lentiviral transduction (MOI 20), bar=50 μ m. (**a**) Loading with lentivirus (LV)/PEI complexes of 0.04 μ g Fe/VP (LV/PEI (0.04)), (**b**) 0.04 μ g Fe/VP NDT (LV/NDT (0.04)), (**c**) 25 μ g Fe/cell PEI (PEI (25)), (**d**) 25 μ g Fe/cell NDT (NDT (25)), (**e**) 25 μ g Fe/cell NDT + 0.04 μ g Fe/VP PEI (NDT (25) + LV/PEI (0.04)), (**f**) unlabeled bPAECs. (**g**) Cell labeling efficiency quantified with the magnetic rack 72 h after magnetic labelling. * $p < 0.05$ vs NDT (25). (**h**) Time course of the normalized turbidity of cell suspensions with bPAECs 72 h after labeling with NDT (25), PEI (25) or NDT (25) + LV/PEI (0.04) (i.e. 3.5 μ g Fe/cell). (**i**) Iron content of bPAECs 72 h after magnetic labeling with NDT or PEI with or without lentiviral transduction obtained by magnetic particle spectroscopy (LV/PEI (0.04), LV/NDT (0.04)) or magnetic responsiveness measurements (PEI (25), NDT (25), NDT (25) + LV/PEI (0.04)), * $p < 0.05$ vs NDT (25).



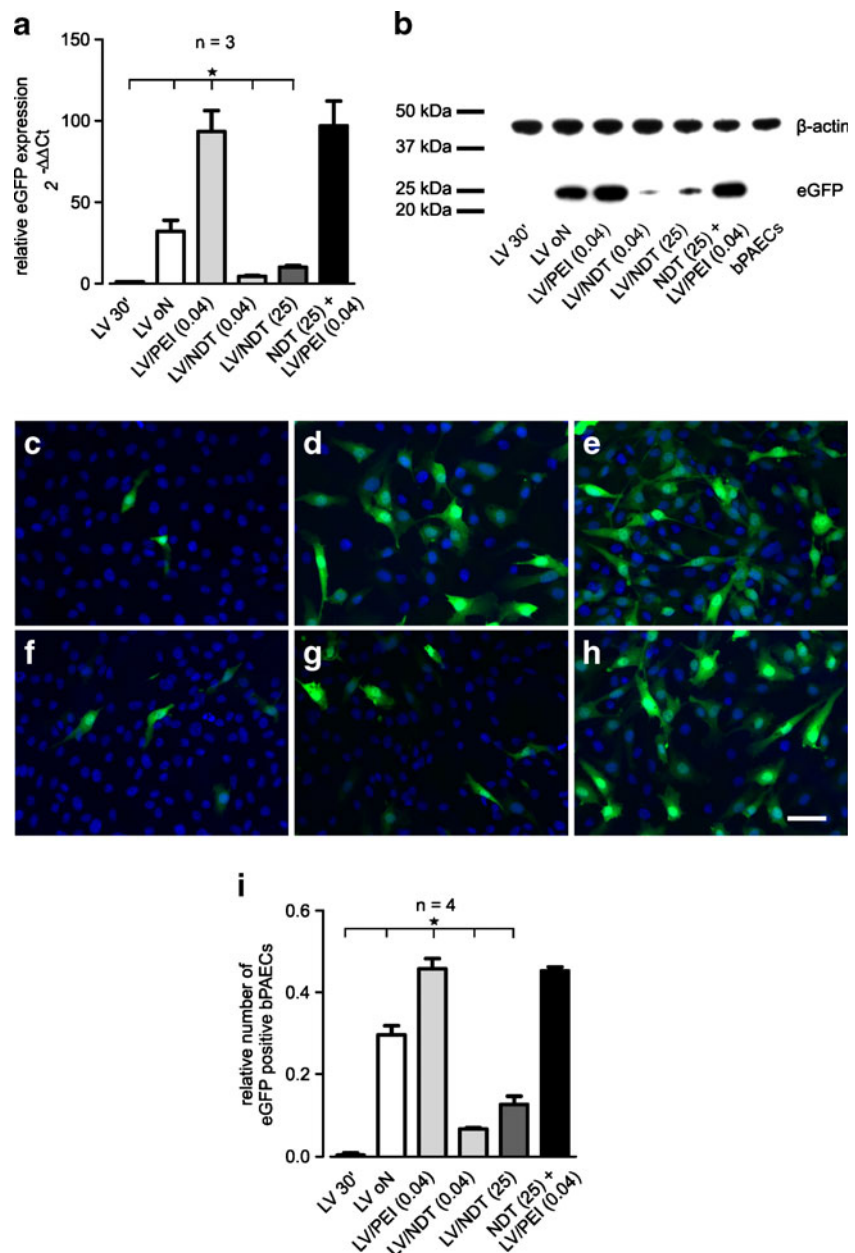
Mag1 + 0.04 μ g Fe/VP PEI-Mag2: $45.3 \pm 1.0\%$, $p > 0.05$ vs 0.04 μ g Fe/VP PEI-Mag2, Fig. 3i). Importantly, MNP-assisted lentiviral transduction at the conditions used did not show toxic effects as determined in LDH assay (Suppl. Fig. 1). Thus, PEI-Mag2 is superior to NDT-Mag1 to obtain an efficient gene and protein expression after lentiviral transduction.

Retention of ECs at the Vascular Wall Under Flow Conditions After Pre-loading and Lentiviral Transduction

To test if the loading of bPAECs with 25 μ g Fe/cell NDT-Mag1 and subsequent transduction with 0.04 μ g Fe/VP PEI-Mag2 affects the expression of endothelial genes and

vascular function we performed qRT-PCR experiments, immunostainings and angiogenesis assays. QRT-PCR analyses showed that lentiviral transduction with the eGFP virus and/or MNP loading did not change eNOS expression in bPAECs (Fig. 4a). Accordingly, we found in immunostainings that endothelial nitric oxide synthase (eNOS, red) and platelet endothelial cell adhesion protein (PECAM, magenta) expression remained unaltered by lentiviral transduction without MNPs or with 25 μ g Fe/cell NDT-Mag1 pre-loading and subsequent 0.04 μ g Fe/VP PEI-Mag2 transduction (Fig. 4b-m). Finally, the angiogenic capacity of bPAECs was found to remain preserved after magnetofection with 25 μ g Fe/cell NDT-Mag1 and 0.04 μ g Fe/VP PEI-Mag2, because eGFP positive cells formed vascular

Fig. 3 Assessment of gene and protein expression in bPAECs after magnetic pre-loading and lentiviral transduction with LV/MNP complexes **(a)** EGFP expression 72 h after transduction (MOI 20) analyzed by qRT-PCR, controls are LV without MNPs for 30 min (LV 30') and LV over night (LV oN), * $p < 0.05$ vs LV/PEI (0.04). **(b)** EGFP expression 72 h after transduction analyzed by Western Blot. **(c-h)** Fluorescence pictures of bPAECs 72 h after lentiviral transduction (MOI 20) with a CMV-eGFP virus, green = eGFP, blue = Hoechst, bar = 100 μm . **(c)** LV 30', **(d)** LV oN, **(e)** LV/PEI (0.04) (i.e. 3.5 pg Fe/cell), **(f)** LV/NDT (0.04), **(g)** LV/NDT (25), **(h)** NDT (25) + LV/PEI (0.04). **(i)** Transduction efficiency quantified by counting of eGFP positive bPAECs, * $p < 0.05$ vs PEI (0.04).



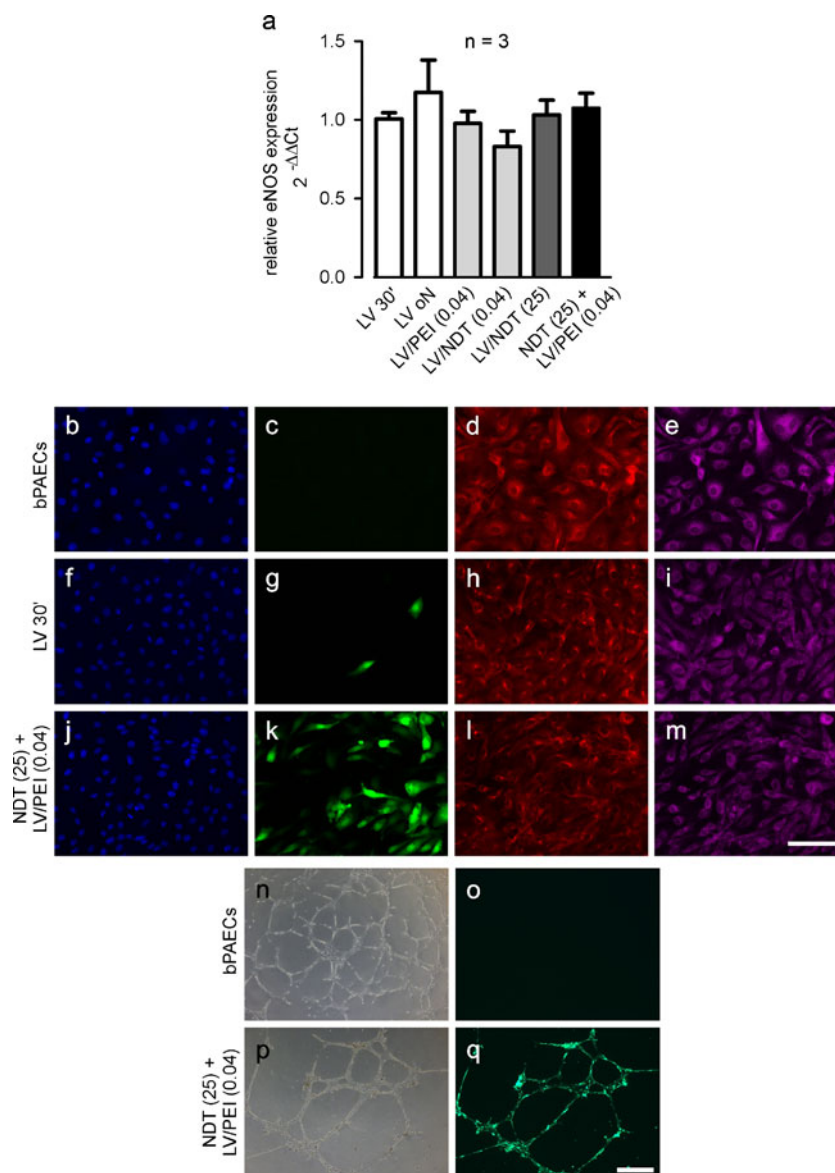
networks in matrigel (Fig. 4n-q). The experiments reveal that EC biology remains intact after magnetic cell labeling with NDT-Mag1 and lentiviral transduction with LV/PEI-Mag2 complexes. Next, we examined if bPAECs loaded with 25 pg Fe/cell NDT-Mag1 and transduced with 0.04 pg Fe/VP PEI-Mag2 could be trapped by a magnetic gradient field under flow conditions. For this purpose magnetically labeled eGFP positive cells were injected into our flow loop system (15) and perfused through a murine aorta with a flow of 4.5 ml/min (Fig. 5a). Two small magnets were positioned adjacent to the vessel to retain the cells at the vascular wall (Fig. 5b-e). Prussian blue staining of the sections revealed the iron content of the retained cells (Fig. 5f) and immunohistochemical stainings demonstrated the co-

expression of PECAM (red) and eGFP (green) (Fig. 5g). These experiments show that pre-loading of bPAECs with 25 pg Fe/cell NDT-Mag1 followed by lentiviral transduction with 0.04 pg Fe/VP PEI-Mag2 enables site-specific deposition of genetically modified ECs at the vascular wall under flow conditions.

Transfer of Therapeutically Relevant Genes by Pre-loading and Lentiviral Transduction

To determine if also therapeutically relevant genes can be efficiently overexpressed after pre-loading with 25 pg Fe/cell NDT-Mag1 and lentiviral transduction with 0.04 pg Fe/VP PEI-Mag2 we used a CMV-eNOS-IRES-eGFP expression

Fig. 4 Cell biological characteristics of bPAECs after magnetic pre-loading and lentiviral transduction with LV/MNP complexes **(a)** eNOS expression 72 h after cell labeling and/or lentiviral transduction analyzed by qRT-PCR. **(b-m)** Immunostaining of bPAECs with or without lentiviral transduction with an eGFP virus, MOI 20. Green = eGFP, red = eNOS, magenta = PECAM, bar = 100 μ m. **(b-e)** native bPAECs, **(f-i)** LV 30', **(j-m)** NDT (25) + LV/PEI (0.04). **(n-q)** Phase contrast and fluorescence pictures of vascular network formation in Matrigel, n=3, bar=500 μ m, **(n,o)** native bPAECs, **(p,q)** bPAECs loaded with NDT (25) + LV/PEI (0.04).

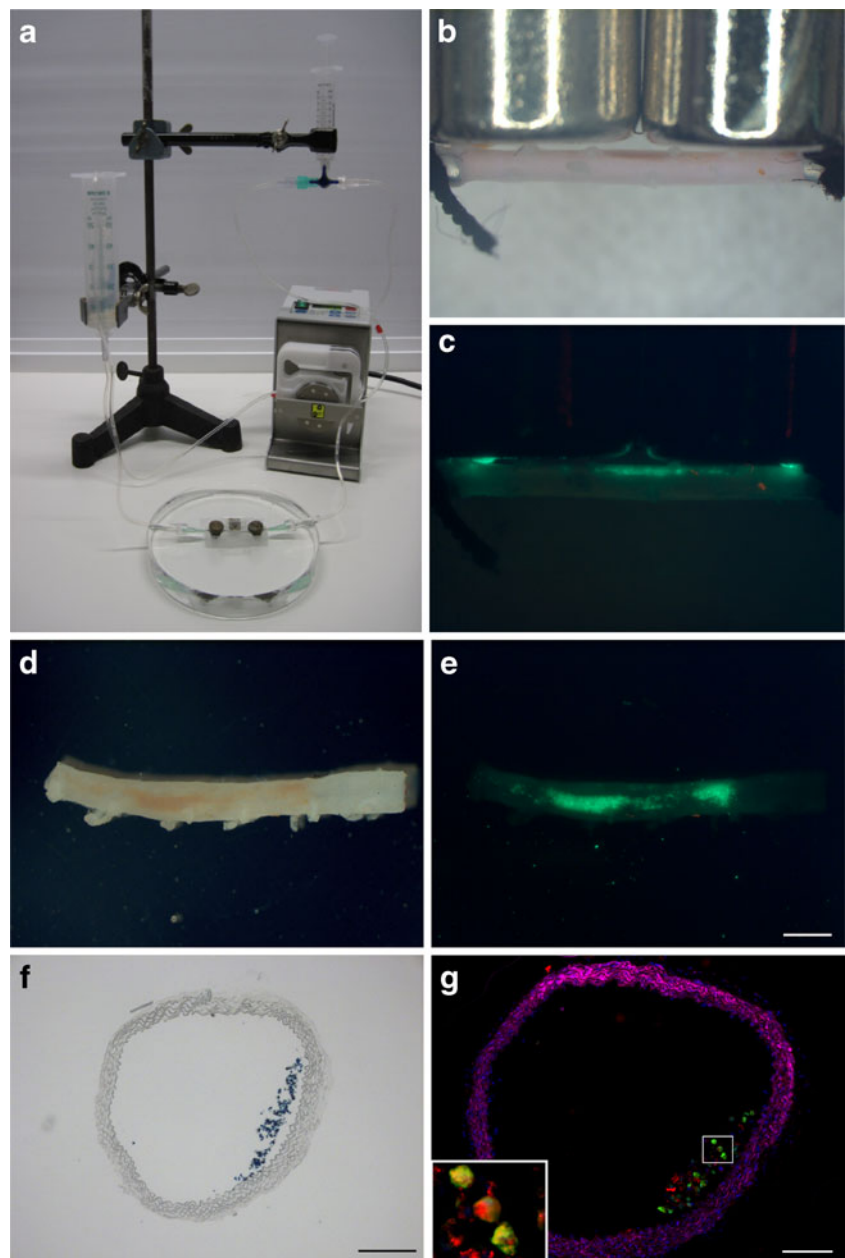


cassette. Similar to our transduction results with the CMV-eGFP reporter virus, 0.04 pg Fe/VP PEI-Mag2 strongly increased eGFP expression ($15.5 \pm 1.7\%$ eGFP positive cells, $p < 0.05$ vs controls). Also with this construct NDT-Mag1 was less efficient. As expected, pre-loading of bPAECs with 25 pg Fe/cell NDT-Mag1 did not reduce the number of eGFP expressing cells after transduction with 0.04 pg Fe/VP PEI-Mag2 complexes: $13.3 \pm 1.4\%$, $p > 0.05$ vs 0.04 pg Fe/VP PEI-Mag2 (Fig. 6a-g). We estimated the eNOS expression of bPAECs by immunostainings and could confirm that eGFP positive cells displayed higher intensity of eNOS signals than eGFP negative cells (Fig. 6h-s, arrows). Since immunostaining does not provide detailed quantitative or functional information, we next determined the functional eNOS expression by measuring nitric oxide production with the fluorescent nitric oxide indicator DAF. We found that 100,000 native bPAECs

produced 966.0 ± 24.4 arbitrary units (AU) of nitric oxide and that this value remained stable during a treatment of 30 min with CMV-eNOS alone or with the iron amount corresponding to 25 pg Fe/cell NDT-Mag1 + 0.04 pg Fe/VP PEI-Mag2 alone; application of the nitric oxide donor sodium nitroprusside was used as positive control and we measured a clear increase of nitric oxide levels. Most importantly, pre-loading of bPAECs with 25 pg Fe/cell NDT-Mag1 and subsequent lentiviral transduction with 0.04 pg Fe/VP PEI-Mag2 complexes led to a significantly elevated nitric oxide production of 1279.7 ± 81.2 AU compared to controls ($p < 0.05$ vs controls), (Fig. 6t).

Thus, pre-loading of bPAECs with NDT-Mag1 particles and subsequent transduction with an eNOS expression cassette using LV/PEI-Mag2 complexes results in eNOS overexpression in cells and enhanced nitric oxide production.

Fig. 5 Retention of bPAECs under flow conditions after magnetic pre-loading and lentiviral transduction with LV/MNP complexes. **(a)** Ex vivo flow loop system where bPAECs after magnetic pre-loading with NDT (25) and transduction with LV/PEI (0.04) complexes were perfused through a murine aorta for 30 min with two small magnets positioned at one side of the vessel. **(b) + (c)** Transmission light and fluorescence pictures of the aorta directly after perfusion with the adjacent magnets, bar=1,000 μm . **(d) + (e)** Transmission light and fluorescence pictures of the aorta after release from the cannulas. **(f)** Prussian blue staining of a cryosection of the perfused aorta, bar=200 μm . **(g)** Fluorescence picture of a cryosection, green = eGFP, red = PECAM, magenta = α -smooth-muscle-actinin, bar=100 μm ; the inset shows overlap of eGFP and PECAM staining; note accumulation of magnetically labeled bPAECs at the site adjacent to the magnet.



DISCUSSION

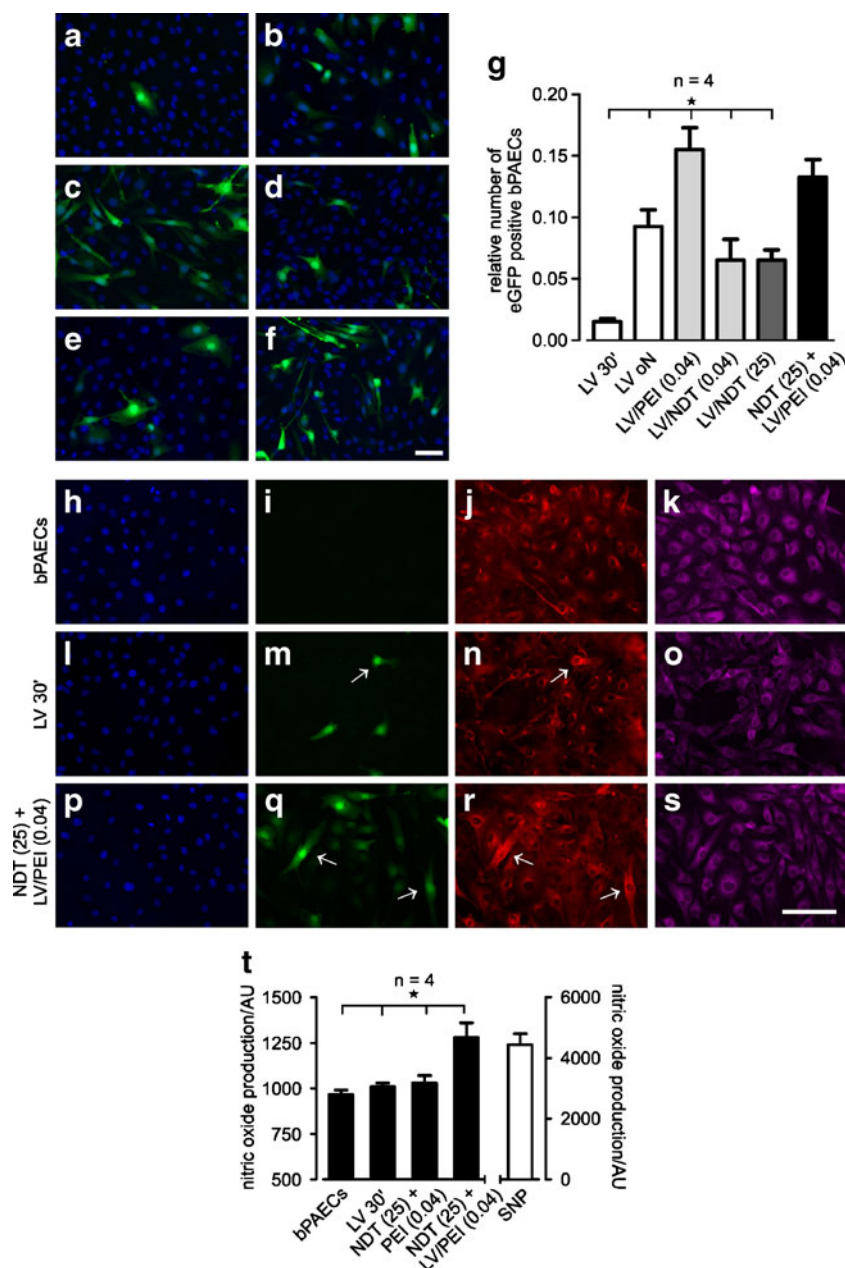
Labeling of ECs by MNPs and their site-specific positioning by magnetic fields may be a promising approach for vascular cell replacement or seeding of the cells on vascular grafts. In addition, MNPs can be used to transfer genes into the target cells.

In our present work we examined a combination of both strategies, which could be particularly helpful in vascular disease. In fact, the herein developed approach may enable the local replacement of damaged ECs by new ECs overexpressing functional genes such as eNOS. However, a single MNP type is not well-suited for both, magnetic cell labeling and lentiviral transduction.

Therefore, we aimed at combining different MNP types for optimal lentiviral transduction and efficient site-specific positioning of these cells under flow conditions. For efficient lentiviral transduction, MNPs that display a high LV binding capacity appear promising. For that reason we tested PEI-Mag2 particles demonstrating maximal virus binding at a low MNP to virus ratio of 0.04 pg Fe/VP. Our findings are in full agreement with data from Trueck *et al.* who showed that PEI-Mag2 applied for lentiviral transduction strongly enhanced gene expression in a broad spectrum of endothelial cells (Trueck, Zimmermann *et al.*, this issue); this type of MNPs proved also much better than NDT-Mag1 for the lentiviral transduction of bPAECs.

For magnetic cell loading both high uptake of MNPs by the cells and a high saturating magnetization of MNPs are

Fig. 6 Assessment of lentiviral transduction efficiency in bPAECs with the therapeutically relevant gene eNOS after magnetic pre-loading and lentiviral transduction with LV/MNP complexes. **(a–f)** Fluorescence pictures of bPAECs 72 h after MNP-assisted lentiviral transduction with a CMV-eNOS-IRES-eGFP expression cassette (MOI 20) with or without magnetic pre-loading, green = eGFP, blue = Hoechst, bar = 100 μ m. **(a)** LV 30', **(b)** LV oN, **(c)** LV/PEI (0.04), **(d)** LV/NDT (0.04), **(e)** LV/NDT (25), **(f)** NDT (25) + LV/PEI (0.04). **(g)** Transduction efficiency quantified by counting of eGFP positive bPAECs, * $p < 0.05$ vs LV/PEI (0.04). **(h–s)** Immunostaining of bPAECs with or without lentiviral transduction with a CMV-eNOS-IRES-eGFP virus. Green = eGFP, red = eNOS, magenta = PECAM, arrows indicate transduced cells with pronounced eNOS expression, bar = 100 μ m **(h–k)** native bPAECs, **(l–o)** LV 30', **(p–s)** NDT (25) + LV/PEI (0.04). **(t)** Nitric oxide production of bPAECs 72 h after magnetic labeling and/or lentiviral transduction with a CMV-eNOS expression cassette. Sodium nitroprusside (SNP) was used as positive control with values on right axis, * $p < 0.05$ vs NDT (25) + PEI (0.04).



essential. Here and in a previous publication (16) NDT-Mag1 particles matched these criteria. We therefore loaded bPAECs with 25 pg Fe/cell NDT-Mag1, a concentration that was found to be non-toxic for bPAECs in a LDH assay and was reported to yield the highest net content at an optimal ratio of applied to internalized iron (16). When we compared iron uptake of NDT-Mag1 in bPAECs with that reported in H441 cells, the iron content turned out to be lower in bPAECs. This may be either due to cell type-dependent nanoparticle uptake characteristics and/or the later time point of analysis in our experiments causing a dilution of iron content over time. In contrast to PEI-Mag2, NDT-Mag1-dependent transduction efficiency was very low and this may be explained by a reduced virus binding

capacity and the lack of proton buffering polyamines that are known to increase endosomal release of complexes with PEI-coated particles (23). Interestingly, pre-loading of bPAECs with NDT-Mag1 particles did not enhance the transduction efficiency with LV/PEI-Mag2 complexes when compared to complexes alone. This is different from findings for magselectofection, where cells attached to beads displayed higher transduction rates on a magnet activated cell sorting (MACS) column loaded with LV/MNP complexes than after standard magnetofection (24). This difference suggests that in our experimental settings the interaction of LV/MNP complexes with the cells is optimally enhanced by the magnetic plate and cannot be further improved by pre-loading with MNPs. The application of an

expression cassette containing the functional gene eNOS and the reporter gene eGFP resulted in a lower transduction efficiency compared to the reporter gene alone, which is likely due to the larger size of the expression cassette. Moreover, the ratio of physical to biological virus titers was higher for LV containing the eNOS-IRES-eGFP plasmid compared to LV with the eGFP cassette alone. Therefore, transduction with 0.04 pg Fe/VP PEI-Mag2 complexes containing the eNOS construct at MOI 20 offered a higher iron amount relative to the number of bPAECs (22.8 pg Fe/cell *vs* 3.5 pg Fe/cell for CMV-eGFP). Nevertheless, this iron mass of PEI-Mag2 particles did not produce efficient magnetic cell labeling and therefore pre-loading with NDT-Mag1 was still necessary.

While previous applications with MNPs either aimed at gene transfer in cells or seeding of cells onto synthetic vascular grafts herein we established a method where we combine gene therapy and endothelial cell replacement under flow conditions. Our approach appears especially promising for the vascular system because injured sites are easily accessible via the blood stream and functional cell replacement is required in different vascular diseases like hypertension or atherosclerosis. Future studies need to prove that this new method provides long-term engraftment of endothelial cells under flow conditions *in vivo* and a functional improvement of vascular tone regulation. When small cell types are used site-specific positioning of genetically engineered cells by magnetic forces may also be applicable for other organ systems.

ACKNOWLEDGMENTS & DISCLOSURES

We thank Dr. Peter Newman (University of Wisconsin) for providing a PECAM antibody and Dr. Christian Plank for helpful discussion. Funding was provided to the junior research group “Magnetic nanoparticles (MNPs)—endothelial cell replacement in injured vessels” by the Ministry of Innovation, Science, Research and Technology of the State of North Rhine-Westphalia (DW) and the DFG Research Unit FOR 917 Nanoguide (AP, CP, BKF, LT).

REFERENCES

- Oghabian MA, Farahbakhsh NM. Potential use of nanoparticle based contrast agents in MRI: a molecular imaging perspective. *J Biomed Nanotechnol*. 2010;6(3):203–13.
- Zhang C, Jugold M, Woenne EC, Lammers T, Morgenstern B, Mueller MM, Zentgraf H, Bock M, Eisenhut M, Semmler W, Kiessling F. Specific targeting of tumor angiogenesis by RGD-conjugated ultrasmall superparamagnetic iron oxide particles using a clinical 1.5-T magnetic resonance scanner. *Cancer Res*. 2007;67(4):1555–62.
- Thiesen B, Jordan A. Clinical applications of magnetic nanoparticles for hyperthermia. *Int J Hyperthermia*. 2008;24(6):467–74.
- Chomoucka J, Drbohlavova J, Huska D, Adam V, Kizek R, Hubalek J. Magnetic nanoparticles and targeted drug delivering. *Pharmacol Res*. 2010;62(2):144–9.
- Saiyed ZM, Parasramka M, Telang SD, Ramchand CN. Extraction of DNA from agarose gel using magnetic nanoparticles (magnetite or Fe₃O₄). *Anal Biochem*. 2007;363(2):288–90.
- Bele M, Hribar G, Campelj S, Makovec D, Gaberc-Porekar V, Zorko M, Gaberscek M, Jamnik J, Venturini P. Zinc-decorated silica-coated magnetic nanoparticles for protein binding and controlled release. *J Chromatogr B Analyt Technol Biomed Life Sci*. 2008;867(1):160–4.
- Mandal SM, Ghosh AK, Mandal M. Iron oxide nanoparticle assisted purification and mass spectrometry based proteolytic mapping of intact CD4⁺ T cells from human blood. *Prep Biochem Biotechnol*. 2009;39(1):20–31.
- Pankhurst QA, Connolly J, Jones SK, Dobson J. Applications of magnetic nanoparticles in biomedicine. *J Phys*. 2003;36:167–81.
- Ito A, Takizawa Y, Honda H, Hata K, Kagami H, Ueda M, Kobayashi T. Tissue engineering using magnetite nanoparticles and magnetic force: heterotypic layers of cocultured hepatocytes and endothelial cells. *Tissue Eng*. 2004;10(5–6):833–40.
- Perea H, Aigner J, Heverhagen JT, Hopfner U, Wintermantel E. Vascular tissue engineering with magnetic nanoparticles: seeing deeper. *J Tissue Eng Regen Med*. 2007;1(4):318–21.
- Pislaru SV, Harbuzariu A, Agarwal G, Witt T, Gulati R, Sandhu NP, Mueske C, Kalra M, Simari RD, Sandhu GS. Magnetic forces enable rapid endothelialization of synthetic vascular grafts. *Circulation*. 2006;114(1 Suppl):1314–8.
- Scherer F, Anton M, Schillinger U, Henke J, Bergemann C, Kruger A, Gansbacher B, Plank C. Magnetofection: enhancing and targeting gene delivery by magnetic force *in vitro* and *in vivo*. *Gene Ther*. 2002;9(2):102–9.
- Chorny M, Polyak B, Alferiev IS, Walsh K, Friedman G, Levy RJ. Magnetically driven plasmid DNA delivery with biodegradable polymeric nanoparticles. *FASEB J*. 2007;21(10):2510–9.
- del Pino P, Munoz-Javier A, Vlskou D, Rivera GP, Plank C, Parak WJ. Gene silencing mediated by magnetic lipospheres tagged with small interfering RNA. *Nano Lett*. 2010;10(10):3914–21.
- Hofmann A, Wenzel D, Becher UM, Freitag DF, Klein AM, Eberbeck D, Schulte M, Zimmermann K, Bergemann C, Gleich B, Roell W, Weyh T, Trahms L, Nickenig G, Fleischmann BK, Pfeifer A. Combined targeting of lentiviral vectors and positioning of transduced cells by magnetic nanoparticles. *Proc Natl Acad Sci USA*. 2009;106(1):44–9.
- Mykhaylyk O, Steingotter A, Perea H, Aigner J, Botnar R, Plank C. Nucleic acid delivery to magnetically-labeled cells in a 2D array and at the luminal surface of cell culture tube and their detection by MRI. *J Biomed Nanotechnol*. 2009;5(6):692–706.
- Mykhaylyk O, Zelphati O, Rosenecker J, Plank C. siRNA delivery by magnetofection. *Curr Opin Mol Ther*. 2008;10(5):493–505.
- Wilhelm C, Billotey C, Roger J, Pons JN, Bacri JC, Gazeau F. Intracellular uptake of anionic superparamagnetic nanoparticles as a function of their surface coating. *Biomaterials*. 2003;24(6):1001–11.
- Gleich B, Weizenecker J. Tomographic imaging using the nonlinear response of magnetic particles. *Nature*. 2005;435(7046):1214–7.
- Pfeifer A, Hofmann A. Lentiviral transgenesis. *Methods Mol Biol*. 2009;530:391–405.

21. Livak KJ, Schmittgen TD. Analysis of relative gene expression data using real-time quantitative PCR and the 2(-Delta Delta C (T)) Method. *Methods*. 2001;25(4):402–8.
22. Wenzel D, Knies R, Matthey M, Klein AM, Welschoff J, Stolle V, Sasse P, Roll W, Breuer J, Fleischmann BK. Beta(2)-adrenoceptor antagonist ICI 118,551 decreases pulmonary vascular tone in mice via a G(i/o) protein/nitric oxide-coupled pathway. *Hypertension*. 2009;54(1):157–63.
23. Sonawane ND, Szoka Jr FC, Verkman AS. Chloride accumulation and swelling in endosomes enhances DNA transfer by polyamine-DNA polyplexes. *J Biol Chem*. 2003;278(45):44826–31.
24. Sanchez-Antequera Y, Mykhaylyk O, van Til NP, Cengizeroglu A, de Jong JH, Huston MW, Anton M, Johnston IC, Pojda Z, Wagemaker G, Plank C. Magslectofection: an integrated method of nanomagnetic separation and genetic modification of target cells. *Blood*. 2011;117(16):e171–81.